

# Quantitative photoacoustic integrating sphere (QPAIS) platform for absorption coefficient and Grüneisen parameter measurements: Demonstration with human blood



Yolanda Villanueva-Palero, Erwin Hondebrink, Wilma Petersen, Wiendelt Steenbergen\*

Biomedical Photonic Imaging Group, MIRA Institute for Biomedical Technology and Technical Medicine, University of Twente, PO Box 217, 7500 AE Enschede, The Netherlands

## ARTICLE INFO

### Article history:

Received 31 March 2016  
Received in revised form 24 February 2017  
Accepted 18 March 2017  
Available online 24 March 2017

### Keywords:

Photoacoustics  
Absorption coefficient  
Grüneisen parameter  
Integrating sphere  
Quantitative photoacoustics  
Human blood

## ABSTRACT

Quantitative photoacoustic imaging in biomedicine relies on accurate measurements of relevant material properties of target absorbers. Here, we present a method for simultaneous measurements of the absorption coefficient and Grüneisen parameter of small volume of liquid scattering and absorbing media using a coupled-integrating sphere system which we refer to as quantitative photoacoustic integrating sphere (QPAIS) platform. The derived equations do not require absolute magnitudes of optical energy and pressure values, only calibration of the setup using aqueous ink dilutions is necessary. As a demonstration, measurements with blood samples from various human donors are done at room and body temperatures using an incubator. Measured absorption coefficient values are consistent with known oxygen saturation dependence of blood absorption at 750 nm, whereas measured Grüneisen parameter values indicate variability among five different donors. An increasing Grüneisen parameter value with both hematocrit and temperature is observed. These observations are consistent with those reported in literature.

© 2017 University of Twente. Published by Elsevier GmbH. This is an open access article under the CC BY-NC-ND license (<http://creativecommons.org/licenses/by-nc-nd/4.0/>).

## 1. Introduction

Quantitative photoacoustic imaging (QPAI) in biomedicine aims at determining target chromophore concentrations such as endogenous hemoglobin in human blood or exogenous contrast agent levels [1]. Accurate measurement of concentrations can be obtained from the absorption coefficient  $\mu_a$  of absorbers of known molar extinction coefficients. In PA images,  $\mu_a$  can be accurately measured if the Grüneisen parameter  $\Gamma$  of the target chromophores is known [1]. Current photoacoustic imaging techniques estimate the initial pressure distribution  $\sigma_o$  which is a product of these factors and the fluence distribution  $\Phi$ :  $\sigma_o = \Gamma\mu_a\Phi$  [1]. Accurate measurement of each factor can give a good estimation of  $\sigma_o$  which can lead to contrast on photoacoustic images which has a quantitative interpretation. Reconstruction algorithms usually assume a constant  $\Gamma$  for all target absorbers wherein measurement of  $\sigma_o$  mainly indicates the absorbed optical energy density  $\mu_a\Phi$ . However, different materials have different  $\Gamma$  values since  $\Gamma$  is also directly related to the material's thermodynamic properties such as thermal expansion coefficient  $\beta$ , specific heat  $C_p$ , and speed of sound  $v_s$ , as it is defined as  $\Gamma \equiv \beta v_s^2 / C_p$  [2,3]. For

example, in biological tissues,  $\Gamma$  varies from around 0.14 for blood [4] to 0.80 for fat [5]. Several publications have reported different techniques to measure  $\Gamma$  of biological chromophores [4–6]. However, the experimental setups require absolute detection sensitivity measurements of the optical and acoustic signals and involve stringent alignment between the incident light and target absorber and acoustic detector which may not be very convenient for measuring with liquid samples. In this paper, we present a method for simultaneously measuring  $\mu_a$  and  $\Gamma$  of small volumes of absorbing and scattering liquids injected in a soft transparent tube mounted through two integrating spheres [7]. With integrating spheres as platform, uniform illumination on the target absorber is achieved. Measuring  $\mu_a$  of absorbing samples in a tube inside an integrating sphere is possible even in the presence of scattering. This method of determining  $\mu_a$  is combined with the technique for measuring  $\Gamma$  of target absorbers in photoacoustic setup. The coupled integrating sphere system is referred to as the quantitative photoacoustic integrating sphere (QPAIS). An equation for measuring  $\mu_a$  using the integrating sphere is derived. Details of the experimental setup and procedures are enumerated. Absolute magnitudes of optical energy and pressure are not necessary for determining  $\mu_a$  and  $\Gamma$ ; instead an in situ calibration of the system is done prior to measurement with samples of interest. The use of the system is demonstrated with measurements on human blood samples. Measurements are done at room and body temperatures using an incubator.

\* Corresponding author.

E-mail address: [w.steenbergen@utwente.nl](mailto:w.steenbergen@utwente.nl) (W. Steenbergen).

## 2. Methodology

### 2.1. Double integrating sphere method and experimental setup

The method for measuring  $\Gamma$  of absorbing liquids using an integrating sphere was already published [8] and was also implemented and briefly described in this paper. The main modifications were as follows: (1) the central frequency of the transducer used for photoacoustic detection was 5 MHz, (2) a soft transparent polyethylene tube with inner diameter = 0.58 mm and outer diameter = 0.96 mm was used and (3) another similar integrating sphere with the same physical properties was connected to the one used for photoacoustic measurements so that the absorption coefficient of the absorbing liquid inside the tube could be simultaneously measured using spectrophotometry.

Fig. 1 shows a schematic top view illustration of the coupled integrating sphere setups. For clarity, only the optical sources and detectors are shown. The transducer (Olympus Panametrics NDT V309 5MHZ/0.5 in. 878182), positioned along the z-axis, the amplifier (Panametrics NDT Ultrasonic Preamp 5678) and oscilloscope (200 MHz, 2 GS/s, Tektronix TDS 2022C/24C) used for photoacoustic detection are not shown on the illustration. Details on photoacoustic measurements are given in [8].

A soft polyethylene tube (Portex, Smiths Medical International, Ltd., UK) with inner diameter of 0.58 mm was inserted through small holes on each integrating sphere (Thorlabs IS200) such that the tube was positioned horizontally inside both spheres. The vertical height of the tube was about 4 mm above each sphere center which ensured that light was directly incident on the sphere wall, avoiding direct illumination of the sample.

Absorption measurement was done using an air-filled integrating sphere 1. A halogen lamp (Avantes AvaLight-Hal) light source was fiber-coupled to this integrating sphere while a spectrometer (Avantes AvaSpec 2048) connected to another port on this sphere using a similar fiber optic was used to monitor the variation on the optical output signal.

Photoacoustic measurement of  $\Gamma$  was done using integrating sphere 2 which was filled with water for acoustic matching with the transducer. A pulsed laser source (OpoletteTM 532I) with wavelength of 750 nm, pulse length 7 ns and a pulse repetition frequency of 20 Hz was connected to this second sphere using an optical fiber (Newport, 0.22 NA, core diameter of 1 mm). Photodetectors (Thorlabs DET10A/M-Si detector) were used to monitor the relative input and output light energy. The uniform illumination on the tube was not affected by the introduction of

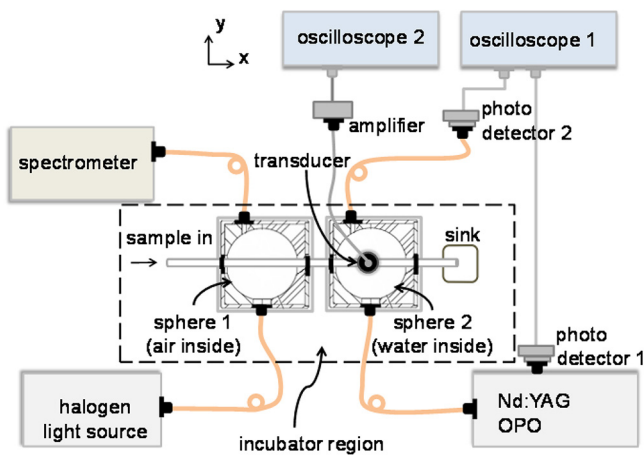


Fig. 1. Top-view schematic diagram of the double integrating sphere setup for measuring absorption coefficient  $\mu_a$  and Grüneisen parameter  $\Gamma$ . The tube is positioned approximately 4 mm above the center plane where the optical ports are located.

water inside the sphere cavity since the sphere wall coating (spectralon material) maintains its high reflectance property even in the presence of water. Moreover, the tube was inserted in a very small hole (with diameter same as the outer diameter of the tube) through the appropriate port plugs such that water did not leak out of the sphere.

For body temperature measurements, the two-integrating sphere setup was placed inside an incubator where ambient temperature adjustments and measurements were possible. A built-in blower warmed the air while a thermal sensor controlled the temperature inside the incubator. It took approximately 10 min to increase from room temperature 22 °C to body temperature of 37 °C. The reservoirs with the medium of interest were also placed inside the incubator so that they were in thermal equilibrium with the entire system during optical and photoacoustic measurements. Another thermal probe (National Instruments NI USB-TC01) was used to monitor and record the temperature measurements. Immediately before absorption and photoacoustic measurements, the air temperature within the incubator, water temperature inside the integrating sphere and temperature of the samples were measured to ensure that they were all in thermal equilibrium. The temperature was monitored throughout the experiments, with the thermal probe positioned close to the tube that goes into integrating sphere 2.

### 2.2. Preparation of human blood samples

Blood samples from healthy donors were obtained from the Experimental Center for Technical Medicine (ECTM) of the University of Twente (UT), which implements proper ethics and approved procedure in utilizing humans and human tissues in research. Blood was directly drawn into vacuum sealed tubes with anticoagulant (either EDTA or heparin) for temporary storage. Immediately before absorption and photoacoustic measurements, blood from each vacuum-sealed tube was pipetted into Eppendorf tubes to obtain three samples from the same donor, each about 1 ml in volume. This step ensured that the oxygen saturation of the hemoglobin in the blood would not abruptly change when blood was injected into the tube in the integrating sphere setup.

Several fresh human blood samples were collected on various days. Measurements were done to investigate the measurable values of  $\mu_a$  and  $\Gamma$  for blood samples (1) drawn from the same donor on various days with new setup calibration (2) drawn from three different donors on the same day with same setup calibration and (3) drawn from various donors on various days with new setup calibration. Absorption and photoacoustic measurements were done within one to two hours after the blood sample was drawn from the donor. Measurements on the same day were done to indicate using the same set of calibration constants for measuring  $\mu_a$  and  $\Gamma$  of blood samples from various donors. On the other hand, measurements on various days implied investigation on the measurable values using new calibration measurements of the system since calibration was always done immediately prior to measurements with the samples of interest.

For hematocrit dependence investigation, whole blood samples inside the vacuum sealed tube were placed in a centrifuge for about 10 min at 2000 rpm until all RBC settled into the bottom of the tube. Plasma and RBC were separated and were pipetted into Eppendorf tubes to obtain about three samples from the same donor, each about 1 ml in volume. Mixtures of red blood cells (RBC) and plasma in varying RBC concentrations (for example, 30 vol% RBC to have hematocrit of approximately 30%) were prepared. Actual hematocrit values were determined by measuring the relative height of the RBC column in capillary tubes.

In order to have absorbing plasma samples at the 750 nm wavelength, small amount of indocyanine green dye solutions (less

than 10 vol%) were added to plasma samples prior to pipetting into Eppendorf tubes to obtain three 1 ml samples from the same donor, which corresponds to bloods samples with zero hematocrit.

### 2.3. $\mu_a$ measurement

Each absorbing sample of interest was injected into the tube until it flowed out the other end to ensure that the same sample was mounted in both integrating spheres. Simultaneous detection of the optical and photoacoustic signals were done in a similar manner as in the calibration measurement.

The absorption coefficient  $\mu_a$  of the absorbing blood sample inside the tube mounted in the integrating sphere 1 was derived using simple energy balance within the sphere. The incident light energy  $E_{in}$  was distributed over and was absorbed by the various parts within the sphere, such that  $E_w$ ,  $E_a$  and  $E_{out}$  are the magnitudes of the absorbed energy by the sphere wall, absorber tube and output port, respectively. From simple energy balance considerations, an equation could be written as follows

$$E_{in} = E_w + E_a + E_{out} \quad (1)$$

Eq. (1) could also be written in terms of the uniform fluence  $\Phi$  within the sphere

$$E_{in} = c_w\phi + c_a\phi + c_o\phi \quad (2)$$

$c_w$ ,  $c_a$  and  $c_o$  depend on the materials used. For the case of a weakly absorbing sample inside the tube (relatively low absorption coefficient which is less than  $2 \text{ mm}^{-1}$ ),  $c_a = \mu_a V$ , such that absorption was uniform over the entire physical volume  $V$ . Using  $E_{out} = c_o\Phi$ , Eq. (2) becomes

$$E_{in} = c_w \frac{E_{out}}{c_o} + \mu_a V \frac{E_{out}}{c_o} + E_{out} \quad (3)$$

Eq. (3) simplifies to

$$\frac{E_{in}}{E_{out}} = a + b\mu_a \quad (4)$$

where  $a = (c_w/c_o) + 1$  and  $b = V/c_o$

Moreover,  $E_{in}$  could be determined using  $E_{out}$  if there is no absorbing sample inside the tube since  $E_{in} = c_{in}E_{out, \text{no absorber}}$ . Also,  $E_{out} = c_{out}E'_{out}$  where  $c_{out}$  is a constant that takes into account experimental factors such as sensitivity of detection and conversion from absolute value to arbitrary units, for example Joules to Counts, as well as the attenuation due to fiber coupling. Thus, Eq. (4) could be written as

$$\frac{E'_{in}}{E'_{out}} = A + B\mu_a \quad (5)$$

where  $E'_{in} = E'_{out, \text{no absorber}}$ , the measured output signal when there is no absorber inside the tube, and  $A$  and  $B$  are constants which could be measured experimentally via a calibration procedure as described above. Rearranging Eq. (5) gives

$$\mu_a = \frac{(E'_{in}/E'_{out}) - A}{B} \quad (6)$$

### 2.4. $\Gamma$ measurement

The corresponding Grüneisen parameter  $\Gamma$  was measured using the following equation [8]

$$\Gamma = \frac{V_{pp}(c + \mu_a V)}{E'_{in, PA} k \mu_a} \quad (7)$$

Here,  $V_{pp}$  was the voltage-peak-to-peak amplitude of the detected photoacoustic signal generated by the absorbing blood

sample with  $\mu_a$  and volume  $V$ .  $\mu_a$  was determined via simultaneous spectrophotometry using integrating sphere 1 as described above, whereas  $V = 0.0134 \text{ cm}^3$ , the physical volume of the tube.  $c$  and  $k$  are the instrument constants determined via the calibration method described in reference [8].  $E'_{in, PA}$  is the relative energy of the incident pulse measured by the photodetector. A detailed derivation of Eq. (7) is given in Ref. [8].

### 2.5. Calibration measurement

A calibration procedure was done to determine the instrument constants. Aqueous ink dilutions were used as absorbers with known  $\mu_a$  values as measured by the standard transmission spectrophotometry technique (Shimadzu UV-VIS). Black Ecoline ink (Royal Talens Ecoline 700 8265) was diluted with deionized and demineralized water in order to make at least five concentrations with  $\mu_a$  values ranging from about  $0.2$  to  $2 \text{ mm}^{-1}$ . Each ink dilution was injected into the tube until it flowed out the other end to ensure that the same absorbing sample was mounted in both integrating spheres. Simultaneous measurements of the optical output and photoacoustic signals were done by synchronizing data collection via computer interface using AvaSpec and LabVIEW software. The AvaSpec software recorded the amount of light reaching the output port of the sphere which was fiber-coupled to the spectrometer that scans a spectrum between  $400 \text{ nm}$  and  $900 \text{ nm}$  wavelengths. With the assumption that only the introduction of the absorbing ink was changed in the integrating sphere system, the relative input light energy  $E'_{in, abs}$  was taken as the detected output signal with only water (no absorbing ink) inside the tube whereas the relative output light energy  $E'_{out, abs}$  was equivalent to the signal with the absorbing ink inside the tube. Absorption other than that due to ink absorption was assumed to be the same in all measurements and can be cancelled out in the calculation for  $\mu_a$  of the absorber in the tube. The necessary constants for measuring  $\mu_a$  of samples were obtained from a plot of  $E'_{in, abs}/E'_{out, abs}$  ratio versus  $\mu_a$  values. On the other hand, the LabVIEW program recorded the temporal photodetector and transducer photoacoustic signals. The area under the curve of the photodetector signal was taken as the relative input energy  $E'_{in, PA}$ , whereas the voltage-peak-to-peak  $V_{pp}$  of the photoacoustic signal was proportional to the initially generated pressure amplitude. To obtain the necessary instrument constants for determining  $\Gamma$ , the measured  $V_{pp}/E'_{in, PA}$  ratio was plotted against corresponding  $\mu_a$  values of ink dilutions. The measured  $\mu_a$  values of the aqueous ink absorbers were used in  $E'_{in}/E'_{out}$  versus  $\mu_a$  and  $V_{pp}/E'_{in, PA}$  versus  $\mu_a$  calibration plots as shown in Figs. 2 and 3.

## 3. Results

Examples of detected photoacoustic signals with ink absorbers and human blood samples are shown in Fig. 2. As can be seen in Fig. 2a, the  $V_{pp}$  amplitude of the signal increases with  $\mu_a$  of the aqueous ink calibration samples. The corresponding  $V_{pp}/E'_{in, PA}$  versus  $\mu_a$  plot is given in Fig. 3b. From this plot, the calibration constants are  $k = 1.17 \text{ m}^3 \text{ s}^{-1}$  and  $c = 3.55 \times 10^{-5} \text{ m}^2$ . Simultaneous with detecting photoacoustic signals, the spectrum of the optical output signal from the second sphere is also measured and the corresponding  $E'_{in}/E'_{out}$  ratio for increasing  $\mu_a$  is given in Fig. 3a. A linear fit on this plot gives  $A = 1.02$  and  $B = 0.21 \text{ mm}^{-1}$ . Immediately after obtaining the calibration data, photoacoustic measurements with blood samples inside the tube are done for several times. Example of the detected signals from whole blood samples is given in Fig. 2b. Each plot corresponds to the average of five measurements averaged from 128 pulses. As a reference, the detected signal with water inside the tube is also given in Fig. 2b. The corresponding  $E'_{in}/E'_{out}$  for blood sample, together with the

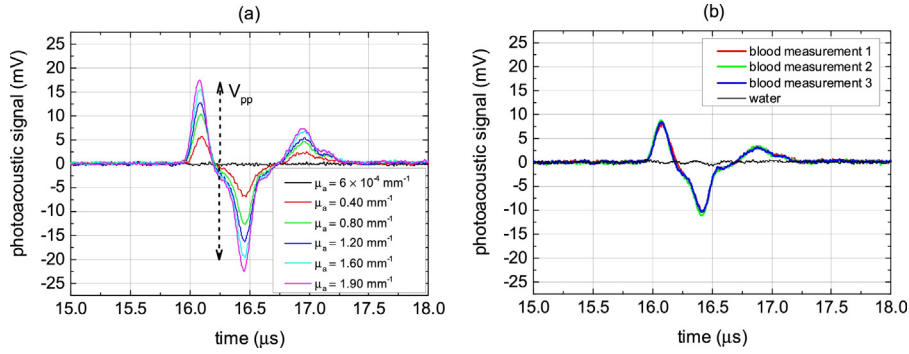


**Fig. 2.** Example of detected photoacoustic signals with (a) aqueous ink dilutions of known  $\mu_a$  and (b) human whole blood sample inside the tube (measured three times). Measurement with water (black line) is shown for reference.

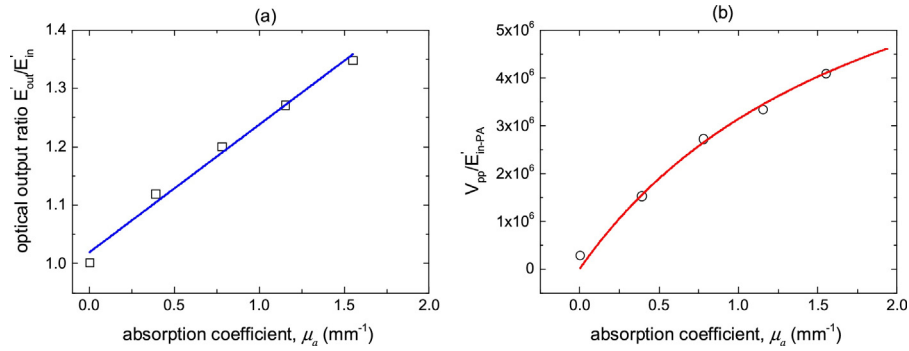


**Fig. 3.** Example of calibration plots for determining the constants (a)  $A = 1.02$  and  $B = 0.21 \text{ mm}^{-1}$  ( $R^2 = 0.99$ ) used for calculating  $\mu_a$  and (b)  $k = 1.17 \text{ m}^3 \text{ s}^{-1}$  and  $c = 3.55 \times 10^{-3} \text{ m}^2$  ( $R^2 = 0.98$ ) for measuring  $\Gamma$ .

calibration constants  $A$  and  $B$  are used in Eq. (7) to determine the  $\mu_{a,\text{blood}}$  of the blood sample. This measured  $\mu_{a,\text{blood}}$ , together with the constants  $k$  and  $c$ ,  $V = 0.0134 \text{ cm}^3$  and corresponding  $V_{pp}/E'_{in,PA}$  are substituted into Eq. (1) to compute  $\Gamma_{\text{blood}}$ .

### 3.1. Measurements with fresh blood samples from the same donor with corresponding setup calibration on various days

Absorption and photoacoustic measurements with fresh blood samples from the same donor are done at various days, using a new calibration of the setup each day. Simultaneous with absorption and photoacoustic measurements, oxygen saturation ( $\text{SO}_2$ ) values of each blood sample are measured using an oximeter (Avoxi-meter). The values given in Table 1 indicate that measurable values of  $\mu_{a,\text{blood}}$  of fresh blood samples from the same donor can change at various days which mainly depend on the oxygen saturation ( $\text{SO}_2$ ) levels. For the highest measured  $\text{SO}_2 = 93\%$ ,  $\mu_{a,\text{blood}} = 0.431 \pm 0.009 \text{ mm}^{-1}$ , whereas for the  $\text{SO}_2 = 46\%$ ,  $\mu_{a,\text{blood}} = 0.807 \pm 0.010 \text{ mm}^{-1}$ , which is consistent with the generally reported value at  $750 \text{ nm}$  [9]. On the other hand, the measured  $\Gamma_{\text{blood}}$  ranges from 0.16 to 0.18 with an average value of  $\Gamma_{\text{blood}} = 0.166 \pm 0.008$ . The standard deviation is only 5% of the average value which indicates that the measurable  $\Gamma$  value for blood samples from the same donor is repeatable. Moreover, the measured

**Table 1**

Measured values of absorption coefficient  $\mu_a$  and Grüneisen parameter  $\Gamma$  for each of the blood samples from the same donor. The absorption and photoacoustic measurements are done on different days and correspondingly with different calibration of the setup. The average  $\Gamma$  value from these three independent measurements is  $\Gamma_{\text{blood}} = 0.166 \pm 0.008$ .

Measurement	$\mu_a$ , $\text{mm}^{-1}$ (mean $\pm$ SD)	$\Gamma$ (mean $\pm$ SD)
1	$0.811 \pm 0.093$	$0.169 \pm 0.008$
2	$0.431 \pm 0.009$	$0.157 \pm 0.003$
3	$0.807 \pm 0.010$	$0.176 \pm 0.002$

value of 0.166 for this human blood sample is only 4% different from the reported value of bovine blood [5].

### 3.2. Measurements with fresh blood samples from different donors with one setup calibration

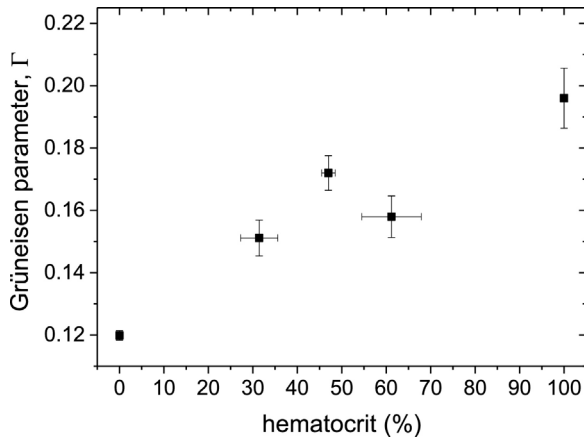
Table 2 shows a summary of the measured  $\mu_{a,\text{blood}}$  and  $\Gamma_{\text{blood}}$  from three different donors (labeled A, B, C) using one set of calibration plots. Three measurements with the same whole blood sample from the same donor are done which gives the standard deviation values. The corresponding hematocrit for each whole blood sample is measured and is also given in Table 2. Measured  $\text{SO}_2$  value ranges from 46% to 84%. The low  $\text{SO}_2$  level indicates that the blood sample is indeed vacuum-sealed and minimally exposed to air from the time it is drawn from the healthy human donor until it is placed into the oximeter. Moreover, the measured  $\mu_{a,\text{blood}}$  varies with the measured  $\text{SO}_2$  values. In particular, as the  $\text{SO}_2$  increases, the measured  $\mu_{a,\text{blood}}$  decreases which is consistent with the reported behavior of  $\mu_a$  at  $750 \text{ nm}$  wavelength [9].

In further investigating the dependence of  $\Gamma_{\text{blood}}$  on hematocrit, Fig. 4 shows a plot of the measured  $\Gamma_{\text{blood}}$  versus hematocrit. For zero hematocrit, measured  $\Gamma_{\text{hct}=0} = 0.120 \pm 0.002$  which is within 10% different from the reported value for bovine serum [5]. As shown in Fig. 4, the measured value of  $\Gamma$  increased to  $0.196 \pm 0.010$  for 100% hematocrit, or the case when there are only erythrocytes inside the tube. The general trend is increasing  $\Gamma$  for increasing hematocrit, except for between 47 and 60 which shows a slight decrease in  $\Gamma$ . Moreover, measurements are done with only the red blood cells (RBC) of the samples drawn from the same donors A, B and C. Table 3 shows the measured values of  $\mu_{a,\text{RBC}}$  and  $\Gamma_{\text{RBC}}$  which are relatively higher than those given in Table 2. The relatively higher values of  $\mu_{a,\text{RBC}}$  can be attributed to the absence of plasma which is mostly (about 90%) water and has relatively low absorption at  $750 \text{ nm}$  wavelength whereas the higher  $\Gamma_{\text{RBC}}$  values can be due to the

**Table 2**

Measured values of oxygen saturation (SO<sub>2</sub>), hematocrit (hct), absorption coefficient  $\mu_a$  and Grüneisen parameter  $\Gamma$  for each of the blood samples from donors A, B and C.

Samples	SO <sub>2</sub> , % (mean $\pm$ SD)	Hematocrit, % (mean $\pm$ SD)	$\mu_a$ , mm <sup>-1</sup> (mean $\pm$ SD)	$\Gamma$ (mean $\pm$ SD)
A	63 $\pm$ 4	49 $\pm$ 2	0.694 $\pm$ 0.026	0.177 $\pm$ 0.005
B	84 $\pm$ 4	46 $\pm$ 1	0.580 $\pm$ 0.016	0.166 $\pm$ 0.006
C	46 $\pm$ 3	47 $\pm$ 1	0.807 $\pm$ 0.010	0.173 $\pm$ 0.002

**Fig. 4.** Measured Grüneisen parameter  $\Gamma$  versus blood hematocrit.**Table 3**

Measured values of absorption coefficient  $\mu_a$  and Grüneisen parameter  $\Gamma$  for samples with 100% hematocrit (containing only red blood cells) from each of the blood samples from donors A, B and C. Three simultaneous absorption and photoacoustic measurements are done for each sample to obtain the standard deviation (SD).

Samples	$\mu_a$ , mm <sup>-1</sup> (mean $\pm$ SD)	$\Gamma$ (mean $\pm$ SD)
A	0.949 $\pm$ 0.022	0.189 $\pm$ 0.006
B	0.818 $\pm$ 0.015	0.207 $\pm$ 0.019
C	0.906 $\pm$ 0.011	0.192 $\pm$ 0.009

modified thermophysical properties of an ensemble of RBC compared to that of whole blood. For example, the thermal expansion coefficient ( $\beta$ ) of RBC is relatively higher than that of whole blood, which is directly proportional to  $\Gamma$ .

### 3.3. Measurements with fresh blood samples from various donors with corresponding setup calibration on various days

The results of the measurements from various donors done on various days are summarized in Table 4. The range of values of measured  $\Gamma$  for fresh human blood samples from five donors varies from 0.141 to 0.177, with a mean value of 0.162 and standard deviation (SD) of 0.016 which is 10% of the mean. It should also be noted that the lowest measured value is within 20% different from the highest measured value, which can indicate a person-to-person variability in  $\Gamma$  that may be attributed to variations in hematocrit and blood composition and condition.

**Table 4**

Measured values of the Grüneisen parameter  $\Gamma$  for blood samples from five different donors (donors D1–D5). Three simultaneous absorption and photoacoustic measurements are done for each sample to obtain the standard deviation (SD).

Samples	$\Gamma$ (mean $\pm$ SD)
D1	0.177 $\pm$ 0.005
D2	0.152 $\pm$ 0.020
D3	0.166 $\pm$ 0.008
D4	0.176 $\pm$ 0.007
D5	0.141 $\pm$ 0.003

### 3.4. Comparison between measurements at room and at body temperatures

Table 5 shows  $\mu_a$  and  $\Gamma$  values of blood samples measured at room (22 °C) and body (37 °C) temperatures. Optical absorption of the samples does not change with temperature. On the other hand, photoacoustic efficiency  $\Gamma$  increased with temperature. For this set of measurements,  $\Gamma$  increased by about 70%, from 0.150  $\pm$  0.011 at 22 °C to 0.245  $\pm$  0.006 at 37 °C. Measurements at 37 °C are done five times. Table 6 shows a summary of measured values for blood samples from five different donors. As noted above, the values of measured  $\mu_a$  change due to the inherent oxygenation level of the blood samples. On the other hand, the average  $\Gamma$  = 0.226  $\pm$  0.015 at 37 °C has 7% standard deviation which indicates that the measured  $\Gamma$  at body temperature also varies minimally relative to mean value, although the lowest measured value of 0.208 is approximately 18% different from the highest measured value of 0.245 which is similar to the difference observed at 22 °C. Comparing the average  $\Gamma$  measured at 37 °C with the one measured at 22 °C, measured  $\Gamma$  increased by about 40% with increased temperature. The increased value of measured  $\Gamma$  can be mainly attributed to the combined increase in the relevant thermal expansion properties of the different components of blood, such as red blood cells and plasma which is mostly water which increases with temperature [3,10]. Furthermore, it is recently reported that the photoacoustic signal from blood samples with varying hematocrit increases with temperature which gives an indication on the temperature dependence of  $\Gamma$  [11].

## 4. Discussion

Prior to performing measurements with blood samples, the influence of light scattering to measurable values of absorption coefficients and Grüneisen parameter of aqueous ink solutions with intralipid was investigated as presented in our paper [12]. Results show that the range of values that can be accurately measured using our integrating sphere method are  $\mu_a < 1.5$  mm<sup>-1</sup> and  $\mu_s' < 3$  mm<sup>-1</sup>, which are within the range of reported values for most biological fluids including blood, at infrared wavelengths. Photoacoustic measurements with these absorbing aqueous ink samples (with and without the intralipid) give values of the Grüneisen parameter close to that of water, as expected since the

**Table 5**

$\mu_a$  and  $\Gamma$  values of blood samples from one donor measured at room (22 °C) and body (37 °C) temperatures.

Temperature (°C)	$\mu_a$ (mm <sup>-1</sup> )	$\Gamma$
22	0.501 $\pm$ 0.028	0.150 $\pm$ 0.011
37	0.493 $\pm$ 0.034	0.245 $\pm$ 0.006

**Table 6**

$\mu_a$  and  $\Gamma$  values of blood samples from five different donors measured at body temperature of 37 °C.

Sample number	$\mu_a$ (mm <sup>-1</sup> )	$\Gamma$
1	0.493 $\pm$ 0.034	0.245 $\pm$ 0.006
2	0.738 $\pm$ 0.003	0.216 $\pm$ 0.005
3	0.497 $\pm$ 0.012	0.208 $\pm$ 0.007
4	0.908 $\pm$ 0.032	0.226 $\pm$ 0.005
5	0.905 $\pm$ 0.012	0.240 $\pm$ 0.005

samples are composed mostly of water. It should be noted that the absorption coefficient can also be measured from the temporal profile of the photoacoustic signal using backward mode detection [13,14]. This photoacoustic measurement of the optical absorption is also investigated for turbid medium using Monte Carlo simulations [15]. In this research, it has been shown that the diameter of the incident laser beam can be chosen such that the absorbed optical energy, which is proportional to the photoacoustic amplitude, is linearly dependent on the absorption coefficient, independent of the scattering coefficient. In our integrating sphere method, the incident light is homogeneously distributed on the absorbing target independent of the beam diameter for  $\mu_a < 1.5 \text{ mm}^{-1}$  and  $\mu'_s < 3 \text{ mm}^{-1}$ .

Absorption and photoacoustic measurements were done on fresh blood samples from healthy human donors. No further analyses on the samples were done to check for similarities and differences in their physiological conditions. Therefore, different measurement scenarios were designed and implemented to investigate the influence of variations in either the blood samples or the experimental setup. Performing measurements on various days (not necessarily at regular intervals) were aimed at investigating on the measurable values of  $\Gamma$  with various fresh blood samples using the integrating sphere setup with new calibration measurement for every sample. This was to investigate the stability of the method and setup and how any perturbation on the system, such as changing the absorbing sample or doing new instrument calibration, could affect the measurable values. Results indicated that the measured  $\mu_a$  changes with blood oxygenation and the measured  $\Gamma$  of blood samples from a particular donor was the same for three independent measurements with a relative error of only 5%.

To investigate further, measurements with more fresh blood samples from various human donors aspirated on different days were performed. Results indicated that the values of measured  $\Gamma$  vary among five different donors with a maximum difference of up to 20%, which is twice the measured experimental error obtained with calibration of the system, as described in [8]. This observation suggested that the  $\Gamma$  of human blood may vary from person to person which depends on physiological factors. Unfortunately, no further analysis on the composition and condition of the obtained blood samples was done. One possible reason for the difference could be the variations in the hematocrit of the samples. However, based on the results of hematocrit dependence measurements shown in Fig. 4, the  $\Gamma$  values of 0.14 and 0.17 would correspond to hematocrits of 20 and 60, respectively, which are beyond the normal range for healthy whole blood. Another possible source for the variation in measured  $\Gamma$  could be the variation in the sample temperature. From the measured average values, an increase from 0.16 at 22 °C to 0.22 at 37 °C implies that 0.004 increase in  $\Gamma$  per degree increase in temperature. This would give a temperature fluctuation of 10 degrees between  $\Gamma = 0.14$  and 0.17, which is very unlikely since the measured ambient temperature during the entire experiment varies within one degree only. Therefore, variations in hematocrit and temperature, although they may have a small effect, were not the main reason for the observed variation in  $\Gamma$  of blood from various human donors. More measurements can be done to explore on the variability of  $\Gamma$  from person-to-person and to further investigate the relevant physiological factors affecting this.

Results shown in Fig. 4 indicated that the measured value of  $\Gamma$  generally increases with blood hematocrit. Blood sample with zero hematocrit corresponds to sample which contains blood plasma and that with 100% hematocrit corresponds to sample which contains only red blood cells. The difference in the values of  $\Gamma$  for these two samples (with zero and 100% hematocrit) could be mainly attributed to the difference in the composition (with different thermophysical properties). For the samples with hematocrit between zero and 100%, the combination of plasma

and red blood cells may have different thermophysical properties which give a different effective  $\Gamma$  values, more red blood cells may indicate higher  $\Gamma$ . It has also been reported (as described in Ref. [16]) that scattering effects could result to higher value of calculated  $\Gamma$ .

The observed variation in  $\Gamma$  with hematocrit and temperature could have consequences for in vivo photoacoustic imaging of microcirculation of blood. Smaller blood vessels tend to have lower hematocrit, the so-called Fahraeus effect, which lowers the effective blood viscosity in the smaller vessels of the microcirculation, especially in neonates [17,18].

The dependence of  $\Gamma$  on blood hematocrit and temperature could form a complication for quantitative photoacoustic imaging, with the aim to determine true absorption coefficients. For example, based on the obtained results, a change in hematocrit values from 50% to 20%, which is found in the microcirculation when comparing blood in large microcirculatory vessels with small vessels, could decrease the Grüneisen parameter by approximately 20%. Furthermore, a five-degree variation of temperature within the body could induce at least 10% variations of the Grüneisen parameter. Such a five-degree temperature difference may exist between the body core and the skin, for instance. Hence, natural variations in local temperature or hematocrit may cause a significant variation in the Grüneisen parameter. Since the photoacoustic stress  $\sigma_o$  is related to  $\Gamma$ ,  $\mu_a$  and optical fluence  $\Phi$  as  $\sigma_o = \Gamma \mu_a \Phi$ , these natural variations in the value of  $\Gamma$  could introduce an extra uncertainty into the problem of quantifying  $\mu_a$ , on top of the uncertainty in fluence  $\Phi$ .

It should also be noted that in our measurements with aqueous ink and blood samples, the difference in acoustic impedance between calibration medium and blood medium was not explicitly considered in the calculations. The polyethylene tube used to mount the sample inside the integrating sphere system was chosen because it has acoustic impedance similar to that of soft biological tissues. Even though the acoustic impedance is not considered in the calculations, the  $\Gamma$  values we obtained are in quite good agreement with that for bovine blood reported in related literature. Moreover, the observations for varying hematocrit and temperature are not affected by a potential difference of acoustic impedance between blood and the calibration medium. Also the variations of  $\Gamma$  between subjects, or between days, are not affected by this.

## 5. Conclusion

A method and system for determining the absorption coefficient  $\mu_a$  and Grüneisen parameter  $\Gamma$  liquid absorbing and scattering samples were designed and implemented using coupled integrating spheres. One sphere was used as a platform for doing absorption measurements and another sphere for photoacoustic measurements with the sample inside a tube mounted simultaneously through both spheres. Using the measured relative optical output ratios, a linear equation for determining  $\mu_a$  was derived based on simple energy balance within the sphere. This measured  $\mu_a$  was used in calculating for  $\Gamma$  of the sample. The application of the developed platform referred as quantitative photoacoustic integrating sphere (QPALS) was demonstrated by measuring  $\mu_a$  and  $\Gamma$  of human blood. At room temperature measurements, for a particular donor, the measured  $\mu_a$  of blood ranged from  $0.807 \text{ mm}^{-1}$  to  $0.431 \text{ mm}^{-1}$  with  $\text{SO}_2$  values of 46% and 93%, respectively and corresponding measured  $\Gamma = 0.166 \pm 0.008$  was repeatable for three independent measurements with new setup calibration at various days. This value is in good agreement with the values obtained for bovine blood [5]. More measurements with fresh blood samples from various donors indicated a decreasing  $\mu_a$  value for increasing blood oxygenation levels which is consistent with that reported in [9]. There was an observed variation in the measured  $\Gamma$  of

blood samples from five human donors, with approximately 20% difference between lowest value 0.141 and highest value 0.177, each within 15% difference from the mean. Measurements with varying blood hematocrit indicated that  $\Gamma$  increases with blood hematocrit. However, the variation in whole blood hematocrit was too small to cause the observed 20% variation in  $\Gamma$ . The blood samples obtained were assumed to be from healthy donors. The actual physiological state of the blood samples and its effect on the measurable  $\Gamma$  could be further investigated. Moreover, measurements at body temperature of 37 °C gave an average  $\Gamma = 0.226 \pm 0.015$  which is about 40% different from the measured value at 22 °C. This observation of increasing  $\Gamma$  value with increasing temperature was consistent with results in Ref. [11].

The shown dependence of Grüneisen parameter on blood hematocrit and temperature could form an extra complication for quantitative photoacoustics, because of the natural variations of hematocrit found in the microcirculation, and temperature differences between the body core and the skin.

The method presented here could be used for measuring with other weakly absorbing liquid samples which are relevant to biomedicine, particularly the target absorbers in photoacoustic imaging. It should be noted that the demonstration of the method was presented here using only one wavelength. In principle, QPAIS could be used with a range of wavelengths such that further quantitative investigations could be done. Additionally, the required incident energy per pulse was relatively low such that the laser source could be changed to a portable laser diode with reasonably short pulse duration. A light source with less energy per pulse (approximately <3 mJ per pulse) could be used, instead of the high energy sources used for photoacoustic imaging.

### Conflict of interest

None declared.

### Acknowledgements

The authors acknowledge The Netherlands Technology Foundation STW for the financial support to this research (Vici grant 10831). Likewise, the authors sincerely appreciate the kind and generous assistance of the Experimental Center for Technical Medicine (ECTM) of the University of Twente, together with the various technicians and donors, who facilitated the supply of fresh human blood samples used in the absorption and photoacoustic measurements.

### References

- [1] B. Cox, et al., Quantitative spectroscopic photoacoustic imaging: a review, *J. Biomed. Opt.* 17 (6) (2012).
- [2] V.E. Gusev, A. Karabutov, *Laser Photoacoustics*, American Institute of Physics, New York, 1993.
- [3] L.V. Wang, H.A. Wu, *Biomedical Optics: Principles and Imaging*, John Wiley & Sons Inc., New Jersey, 2007.
- [4] E.V. Savateeva, et al., Optical properties of blood at various levels of oxygenation studied by time resolved detection of laser-induced pressure profiles, *Biomed. Optoacoust.* III 4618 (2002) 63–75.
- [5] D.K. Yao, et al., Photoacoustic measurement of the Gruneisen parameter of tissue, *J. Biomed. Opt.* 19 (1) (2014).
- [6] B. Soroushian, W.M. Whelan, M.C. Kolios, Study of laser-induced thermoelastic deformation of native and coagulated ex-vivo bovine liver tissues for estimating their optical and thermomechanical properties, *J. Biomed. Opt.* 15 (6) (2010).
- [7] P. Elterman, Integrating-sphere spectroscopy, *J. Opt. Soc. Am.* 59 (11) (1969) 1537.
- [8] Y. Villanueva, et al., Photoacoustic measurement of the Gruneisen parameter using an integrating sphere, *Rev. Sci. Instrum.* 85 (7) (2014).
- [9] N. Bosschaart, et al., A literature review and novel theoretical approach on the optical properties of whole blood, *Lasers Med. Sci.* 29 (2) (2014) 453–479.

- [10] I. Larina, K. Larin, R. Esenaliev, Real-time optoacoustic monitoring of temperature in tissues, *J. Phys. D: Appl. Phys.* 38 (2005) 2633–2639.
- [11] E.V. Petrova, A.A. Oraevsky, S.A. Ermilov, Red blood cell as a universal optoacoustic sensor for non-invasive temperature monitoring, *Appl. Phys. Lett.* 105 (2014).
- [12] Y.Y. Villanueva, C. Veenstra, W. Steenbergen, Measuring absorption coefficient of scattering liquids using a tube inside an integrating sphere, *Appl. Opt.* 55 (15) (2016).
- [13] A. Karabutov, N.B. Podymova, V.S. Letokhov, Time-resolved laser optoacoustic tomography of inhomogeneous media, *Appl. Phys. B* 63 (1996) 545.
- [14] A. Karabutov, et al., Backward mode detection of laser-induced wide-band ultrasonic transients with optoacoustic transducer, *J. Appl. Phys.* 87 (4) (2000).
- [15] I.M. Pelivanov, et al., Opto-acoustic measurement of the local light absorption coefficient in turbid media: 1. Monte-Carlo simulation of laser fluence distribution at the beam axis beneath the surface of a turbid medium, *Quantum Electron.* 39 (9) (2009) 830–834.
- [16] R.K. Saha, M.C. Kolios, Photoacoustic signals from red blood cells, *J. Acoust. Soc. Am.* 129 (5) (2011).
- [17] J.H. Barbee, G.R. Cokelet, The Fahraeus effect, *Microvasc. Res.* 3 (1) (1971) 6–16.
- [18] E.P. Zilow, O. Linderkamp, Viscosity reduction of red blood cells from preterm and full-term neonates and adults in narrow tubes (Fahraeus-Lindqvist effect), *Pediatr. Res.* 25 (6) (1989) 595–599.



**Yolanda Villanueva-Palero** obtained her bachelor of science in applied physics degree from the National Institute of Physics at the University of the Philippines in 2000. She did her bachelor thesis project on holographic optical data encryption in an iron-doped lithium niobate crystal at the Photonics Research group. In December 2003, she also joined a six-month research training program at the former Precision Instrument Development Center of Taiwan Republic of China, where she performed pulsed laser deposition of zinc oxide thin films. She obtained a master of physics degree from the Vrije University Amsterdam in August 2010. Her master thesis was on Casimir-like effect in granular fluids. In January 2016, she obtained her PhD degree at the University of Twente where she developed a quantitative photoacoustic integrating sphere platform for measuring the Grüneisen parameter, optical absorption and fluorescence quantum yield of biomedical fluids, under the supervision of Prof. Wiendelt Steenbergen of the biomedical photonic imaging group.



**Erwin Hondbrink** received his bachelor degree in biomedical electrical engineering in 1998 at Hogeschool Enschede. From 1999 to 2015, he worked almost continuously as a research engineer at the University of Twente. He worked in the Low Temperature group and the Biomedical Imaging group on various research projects in micro cooling, laser doppler, LASCA, photoacoustics and acousto optics. His focus is on software development, data acquisition, vision and electronics. In 2007, he worked at Perimed AB in Sweden on the development of a LASCA system. From 2009 to 2010, he worked at Ostendum BV on a portable biosensor for the detection of bacteria, viruses, yeasts, and biomarkers.



**Wilma Petersen** studied medical laboratory education with the specialization Medical Chemistry and Clinical Chemistry at the Hogeschool Enschede. She received both degrees in 1998. She started working in Academic Medical Center (AMC) in Amsterdam as research analyst where she generated proteins to do structural function analysis. In 2005, she joined the Biomedical Photonic Imaging group at the University of Twente, Enschede where she prepared photoacoustic contrast agents such as goldnanorods that were conjugated with antibodies. Various aspects of these contrast agents were researched and investigated. She is now working on several other projects including the photoacoustic measurement of the Grüneisen parameter using an integrating sphere.



**Wiendelt Steenbergen** obtained a PhD degree in fluid dynamics at the Eindhoven University of Technology in 1995, after which he joined the University of Twente, Enschede (the Netherlands) as a postdoc. In 2000 he was appointed assistant professor in biomedical optics and broadened his scope to low-coherence interferometry and photoacoustic and acousto-optic imaging. In 2010, he became full professor and group leader of the newly formed Biomedical Photonic Imaging group of the University of Twente.